

are bound in crystals only by the very weak van der Waals forces; if we were to ascribe a finite radius to the isolated atom, it would be for the rare gases that such a radius would most nearly equal the crystal radius. Since the corrected statistical model predicts close to these values for the rare-gas atomic radii, it would appear that the correct interpretation of minimum-energy, or

zero boundary pressure, solutions is as representing isolated atoms.

ACKNOWLEDGMENT

The author wishes to express his appreciation to Dr. Robert D. Cowan for reading the manuscript and for his very helpful counsel and suggestions.

Theory of Low-Energy-Electron Scattering by Polar Molecules*

M. H. MITTLEMAN AND R. E. VON HOLDT

Lawrence Radiation Laboratory, University of California, Livermore, California

(Received 11 June 1965)

The diffusion cross section for electrons in a gas of polar molecules is calculated. The improvement over a previous calculation is the use of the exact scattering cross section of a charged particle by a point dipole rather than the first Born approximation. For H₂O the correction amounts to about 20% and worsens the agreement with experiment.

I. INTRODUCTION

IN a paper¹ having a title identical with this one, Altshuler calculated the diffusion cross section for free electrons in a gas of polar molecules. He shows that the coupling among the rotational states of the molecule may be neglected, provided the electron energy is low enough and the dipole strength is not too large. In all practical situations the approximation is a good one and the scattering may then be calculated from a molecule with fixed orientation. The cross section is then averaged over the orientation of the molecule. Altshuler treats the molecule as a point dipole and uses the first Born approximation to obtain his cross section. He then averages quantum-mechanically over the orientation of the dipole. He notes that the result in the first Born approximation is identical with the classical averaging procedure. We should like to point out that this is the case for any dependence of the cross section upon the dipole direction. We have obtained the exact differential cross section for the scattering of a charged particle by a point dipole for a variety of dipole strengths and orientations, and we then obtain the diffusion cross section. In general, the results are higher than the Born approximation. Finally, we estimate the corrections resulting from the short-range potential of the molecule, with results which differ from Altshuler's.

II. QUANTUM MECHANICAL SCATTERING FROM A POINT DIPOLE

Our starting point is the wave equation

$$\left[\nabla^2 + k^2 + \frac{\alpha \cdot \mathbf{r}}{r^3} \right] \psi(\mathbf{r}) = 0, \quad (1)$$

* Work performed under the auspices of the U. S. Atomic Energy Commission.

¹ S. Altshuler, Phys. Rev. **107**, 114 (1957).

where the dimensionless dipole moment α is related to the actual dipole moment \mathbf{D} by

$$\alpha = 2\mathbf{D}/ea_0. \quad (2)$$

The geometry is illustrated in Fig. 1 where k is the incident wave vector and the scattered particle has a unit *negative* charge. Equation (1) is separable in the usual spherical coordinates r , μ , and ϕ , ($\mu = \cos\theta$). With the assumption

$$\psi \sim R(r)\theta(\mu)e^{im\phi},$$

Eq. (1) separates into

$$\left[\frac{d}{d\mu} (1-\mu^2) \frac{d}{d\mu} - \frac{m^2}{1-\mu^2} + \alpha\mu + L_n^m(L_n^m+1) \right] \theta_n^m(\mu) = 0, \quad (3)$$

$$\left[\frac{d^2}{dr^2} + \frac{2}{r} \frac{d}{dr} + k^2 - \frac{L_n^m(L_n^m+1)}{r^2} \right] R_n(r) = 0, \quad (4)$$

where the condition that ψ be single-valued requires that m be an integer. The separation constant is denoted by $L_n^m(L_n^m+1)$. The condition that $\theta_n^m(\pm 1)$ be finite is a restriction upon L_n^m to certain allowed values. The integer n will denumerate these eigenvalues. A solution of Eq. (3) may be obtained by expanding in the complete set P_l^m .

$$\theta_n^m(\mu) = \sum_{q=0}^{\infty} \Delta_{nq}^m P_{q+|m|}^m(\mu) \times \left[\frac{2q+2|m|+1}{2} \frac{q!}{(q+2|m|)!} \right]^{1/2}, \quad (5)$$

where the coefficients and eigenvalues are determined

from the three-term recurrence relation,

$$\begin{aligned} & [L_n^m(L_n^{m+1}) - (q+|m|)(q+|m|+1)]\Delta_n^m \\ & + \alpha \left[\Delta_{n,q+1}^m \left(\frac{(q+1)(q+2|m|+1)}{(2q+2|m|+1)(2q+2|m|+3)} \right)^{1/2} \right. \\ & \left. + \Delta_{n,q-1}^m \left(\frac{q(q+2|m|)}{(2q+2|m|+1)(2q+2|m|-1)} \right)^{1/2} \right] = 0. \end{aligned} \quad (6)$$

The method of solution is described in the Appendix. We merely note here that the normalization can be chosen so that for each m the θ_n^m form a complete orthonormal set.

The solution of the radial Eq. (4) which is finite at the origin is the spherical Bessel function $j_{L_n^m}(kr)$. The condition that this function be finite at the origin places a bound upon the eigenvalue,

$$L_n^m < -\frac{1}{2}, \quad (7)$$

which results in an upper bound on the magnitude of the dipole moment

$$\alpha < 1.279. \quad (7a)$$

Otherwise, the potential is too attractive (in some directions) and no solutions exist.²

Having obtained a general solution of Eq. (1) in the form

$$\psi = \sum_{nm} j_{L_n^m}(kr) \theta_n^m(\mu) e^{im\phi} A_{nm}, \quad (8)$$

the coefficients A_{nm} are determined from the boundary condition

$$\lim_{r \rightarrow \infty} \psi = e^{ik \cdot r} + (e^{ikr}/r) f(\mu, \phi). \quad (9)$$

In order to proceed, we expand the plane wave

$$e^{ik \cdot r} = \sum_{l=0}^{\infty} \sum_{m=-l}^l B_{lm}(kr) \theta_l^m(\mu) e^{im\phi}. \quad (10)$$

We can invert this equation for B_{lm} and use the expansion of the plane wave in spherical Bessel functions to get

$$\lim_{x \rightarrow \infty} B_{lm}(x) = (1/2ix) [\alpha_{lm} e^{ix} - \beta_{lm} e^{-ix}], \quad (11)$$

where

$$\begin{aligned} \left\{ \begin{array}{l} \alpha_{lm} \\ \beta_{lm} \end{array} \right\} &= 2 \sum_{q=0}^{\infty} \Delta_{lq}^m \left(\frac{(2q+2|m|+1)}{2} \frac{q!}{(q+2|m|)!} \right)^{1/2} \\ &\times P_{q+|m|}^m(\eta) \left\{ \begin{array}{l} 1 \\ (-1)^{q+m} \end{array} \right\} = \left\{ \begin{array}{l} \theta_l^m(\eta) \\ (-1)^m \theta_l^m(-\eta) \end{array} \right\}, \end{aligned} \quad (12)$$

where $\eta = \cos \xi$. The condition Eq. (9) then fixes A_{nm}

$$A_{nm} = e^{-i(\pi/2)L_n^m} \beta_{nm} \quad (13)$$

² N. F. Mott and H. S. W. Massey, in *The Theory of Atomic Collisions* (Oxford University Press, London, 1950), 2nd ed., p. 40 describe a similar situation for the $1/r^2$ central potential.

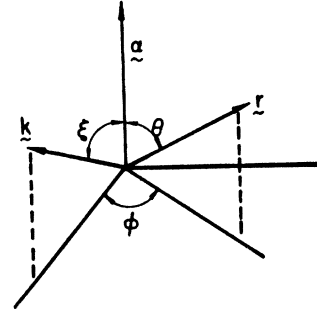


FIG. 1. The geometry of the problem.

and yields

$$\begin{aligned} f(\mu, \phi; \eta, \alpha) &= \frac{i}{2k} \sum_{n=0}^{\infty} \sum_{m=-\infty}^{\infty} \theta_n^m(\mu) e^{im\phi} \\ &\times [\theta_n^m(\eta) - \theta_n^m(-\eta) e^{-i(L_n^m - m)\pi}]. \end{aligned} \quad (14)$$

In this form it is not difficult to show that

$$f(\mu, \phi; \eta, \alpha) = f(-\eta, \phi; -\mu, \alpha). \quad (14a)$$

The differential scattering cross section is, of course, given by

$$\frac{d\sigma}{d\Omega}(\mu, \phi; \eta, \alpha) = |f|^2. \quad (15)$$

The energy dependence k^{-2} , which is exact, was noted by Altshuler in first and second Born approximations. It is simply a consequence of the scaling of Eq. (1). The first Born approximation to Eq. (15) yields

$$\begin{aligned} d\sigma/d\Omega|_B &= (\alpha^2/4k^2) \\ &\times [(\mu - \eta)/(1 - \mu\eta - [(1 - \mu^2)(1 - \eta^2)]^{1/2} \cos \phi)]^2. \end{aligned} \quad (16)$$

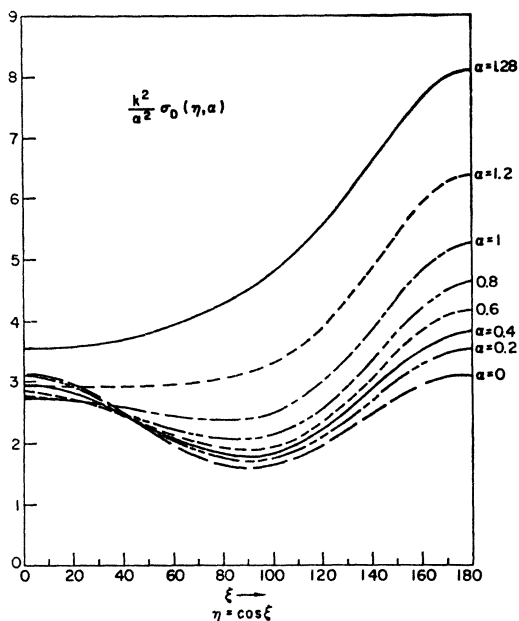
It diverges in the forward direction where it becomes the correct result.³ The result, Eq. (15), is much too complicated to present here; we content ourselves with some general remarks.

For small α ($=0.2$) the exact result is significantly different from Eq. (16). There is more structure in the cross section, but it averages out about Eq. (16). For higher values of α , up to the critical value of 1.279, the results are completely different from the Born result, and in general are higher. There is a more pronounced tendency to peak near the forward direction than for low α .

The momentum transfer, or diffusion cross section, is obtained from Eq. (15) by

$$\sigma_D(\eta, \alpha) = \int d\Omega [1 - \hat{k} \cdot \hat{r}] \frac{d\sigma}{d\Omega}. \quad (17)$$

³ In the forward direction Eq. (16) is indeterminate. The limit we refer to here is $\phi=0, \mu \rightarrow \eta$. The divergence comes from scattering at large distances where the Born approximation becomes correct so that Eqs. (15) and (16) must coincide. Similarly, the total cross section diverges.

FIG. 2. $(k^2/\alpha^2)\sigma_D(\eta, \alpha)$ versus dipole orientation.

In Fig. 2 we have plotted $k^2/\alpha^2\sigma_D$ versus η for various values of the dipole strength, from $\alpha=0$ to the critical value. They may be averaged over the orientation of the dipole,

$$\sigma(\alpha) = \int_{-1}^1 \frac{d\eta}{2} \sigma_D(\eta, \alpha), \quad (18)$$

to give the effective diffusion cross section. In Fig. 3 we have plotted the ratio $\bar{\sigma}(\alpha)/\sigma_B$ versus α . Here σ_B is the Born result

$$\sigma(\alpha)/\alpha^2|_{\alpha=0} = \frac{2}{3}(\pi/k^2). \quad (19)$$

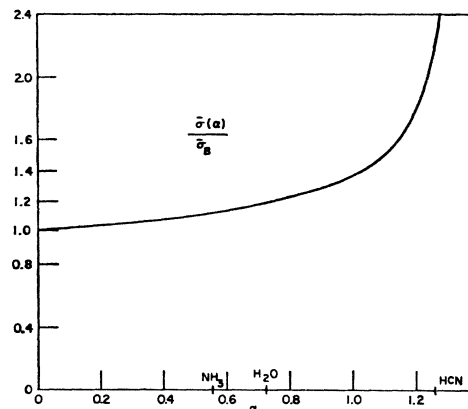
We have indicated the results for several polar molecules on the figure. The Born approximation for NH_3 is about 12% low, for H_2O it is about 20% low, and for HCN more than a factor of 2 too low.

Altshuler presents a comparison with experimental results for NH_3 and H_2O . The chief disagreement with his Born approximation theory is the energy dependence. Our calculation cannot change this. The tendency of our correction is to reduce the agreement with experiment.

Our calculations describe the molecule as a point dipole. We can estimate the correction to this at low energies. Suppose that there is an additional short-range ($=r_0$) potential $\hbar^2/2mU$ and that its effects are small enough to be treated as a perturbation. Then the change in the scattering amplitude is

$$\delta f = -\frac{1}{4\pi} \int d^3r \psi_{-\mathbf{k}'}(r) U(r) \psi_{\mathbf{k}}(r), \quad (20)$$

where \mathbf{k} and \mathbf{k}' are the initial and final scattering

FIG. 3. $\bar{\sigma}(\alpha)/\sigma_B$ versus dipole strength (in units of $\frac{1}{2}ea_0$).

vectors. For low energies ($\hbar r_0 \ll 1$) the change in the diffusion cross section has an energy dependence given by

$$\delta\bar{\sigma} \sim (U/k^4)(\hbar r_0)^{2L_0^0+3}, \quad (21)$$

where L_0^0 is the lowest eigenvalue of the $m=0$, Eq. (3). For H_2O , $\alpha \approx 0.73$ and $L_0^0 \approx 0.14$ so that $\delta\bar{\sigma} \sim k^{-0.72}$. Altshuler quotes a correction which is energy-independent, in contradiction to this.

It is clear that such a perturbation treatment is not valid for $\alpha < 1.279$ since in that case there is no zero-order solution since the approximation of the molecule by a point dipole is invalid.

APPENDIX

For fixed m , α , and n , the recurrence relation Eq. (7) has the form

$$b_{i-1}x_{i-1} + (a_i - \lambda)x_i + b_i x_{i+1} = 0, \quad (i=1, 2, \dots).$$

Thus, x is an eigenvector of an infinite triple-diagonal symmetric matrix A , and λ is the corresponding eigenvalue.

Let M_n be the matrix obtained from A by deleting all but the first n rows and columns, and let $P_n(x)$ be the determinant of $(M_n - xI)$, then

$$P_n(x) = (a_n - x)P_{n-1}(x) - b_{n-1}^2 P_{n-2}(x), \quad (n=1, 2, 3, \dots),$$

with

$$P_{-1}(x) \equiv 0, \quad P_0(x) \equiv 1.$$

As pointed out by Givens,⁴ for nonzero b_n 's the roots of $P_n(x)$ separate the roots of $P_{n+1}(x)$. In our case, b_n/a_n for successive n tends to zero with increasing n , and the least roots become computationally equal. Thus, the first ten roots of P_{19} and P_{20} were identical to eight significant figures. Using the first ten roots of $P_{20}(x)$ as trial eigenvalues of M_{20} , corresponding trial eigenvectors were obtained from Eq. (7) as follows:

⁴ W. Givens, Natl. Bur. Std. (U. S.) Applied Math. Series No. 29, pp. 117-122.

Let the trial roots be ordered such that

$$\lambda_i < \lambda_{i+1}.$$

For $\lambda = \lambda_k$, assume values for x_1 and x_{20} . Generate two sequences, using Eq. (7),

$$x_1, x_2, \dots, x_k$$

and

$$x_{20}, x_{19}, \dots, x_k;$$

then scale one of the sequences such that the two values of x_k are identical.

Each trial eigenvector is improved by repeated appli-

cation of the inverse power method, that is, choose $\lambda \neq \lambda_k$ but λ much closer to λ_k than to any other trial eigenvalue and replace the trial eigenvector \mathbf{x} by the solution of

$$(A - \lambda I)\mathbf{z} = \mathbf{x}.$$

The first ten eigenvectors of M_{20} were normalized to unit length. The trial eigenvalues were replaced by

$$\lambda = (\mathbf{x} \cdot A \mathbf{x}).$$

As a final check, the largest observed dot product of two distinct eigenvectors was less than 10^{-14} .

Electron Capture by High-Energy Deuterons in Gases*

KLAUS H. BERKNER, SELIG N. KAPLAN, GEORGE A. PAULIKAS,[†] AND ROBERT V. PYLE

Lawrence Radiation Laboratory, University of California, Berkeley, California

(Received 9 June 1965)

Measurements of electron-capture cross sections of 12.9- and 21.0-MeV deuterons in He, N₂, and Ar are reported and compared with published theoretical estimates and experimental results for protons with energies ≤ 1 MeV.

I. INTRODUCTION

MANY calculations of cross sections for electron capture by fast protons in gases, especially in atomic hydrogen, have been published. The philosophies of the several approaches are discussed in Refs. 1 through 4 and in the review paper by Bates and McCarroll.⁵ There is substantial disagreement as to both the magnitudes and the energy dependence of the published cross sections for energies > 1 MeV.

We have measured the capture cross sections for 12.9- and 21.0-MeV deuterons in He, N₂, and Ar.⁶ Although these few measurements represent only a beginning, their magnitudes can be checked against the published calculations, and from a comparison with the experimental results of Barnett and Reynolds at proton energies ≤ 1 MeV,⁷ inferences can be drawn about the average energy dependence for protons in the energy range 1 to 10 MeV.

II. APPARATUS AND PROCEDURE

Deuterons from the Berkeley Hilac were deflected 15 deg, collimated to a diameter of 5 mm, and passed through a differentially pumped gas cell 24 cm long. The neutral particles produced in the gas were detected with a 20-mm-diam solid-state detector, pulse-height analyzed, and counted. Charged particles emerging from the gas cell were deflected into a wide-aperture Faraday cup placed in the analyzing magnetic field to eliminate secondary-electron losses. The currents were recorded with a calibrated integrating electrometer.

At full Hilac beam current it was possible for us to locate the charge-exchange-produced neutral beam by observing it on a phosphor-coated Lucite plate. The Hilac intensity was then reduced and the phosphor replaced by the solid-state detector, which easily contained the entire beam. The energies of the deuterons were determined by the deflection in the bending magnet and by pulse-height analysis with a Li-drifted counter and Al foil degraders. The detector was calibrated with an Am²⁴¹ α source. The uncertainty in the energies is $\pm 1.5\%$.

The pressures in the target were measured with a Schulz-Phelps-type ionization gauge, which was calibrated against a liquid-nitrogen-trapped McLeod gauge. We used the results of Meinke and Reich⁸ to correct for the pumping effect of the mercury streaming to the cold trap. The maximum correction was 12%, for the

* Work performed under the auspices of the U. S. Atomic Energy Commission.

[†] Present address: Aerospace Corporation, El Segundo, California.

¹ B. H. Bransden and I. M. Cheshire, Proc. Phys. Soc. (London) **81**, 820 (1963).

² R. A. Mapleton, Phys. Rev. **130**, 1839 (1963).

³ M. H. Mittleman, Proc. Phys. Soc. (London) **81**, 633 (1963).

⁴ R. A. Mapleton, Phys. Rev. **130**, 1829 (1963).

⁵ D. R. Bates and R. McCarroll, Advan. Phys. **11**, 39 (1962).

⁶ Measurements were also made in H₂ but are not reported because of a 0.08% N₂ contamination of the target gas, which necessitated large corrections to the data.

⁷ C. F. Barnett and H. K. Reynolds, Phys. Rev. **109**, 355 (1958).

⁸ Ch. Meinke and G. Reich, Vacuum **13**, 579 (1963).